The tumour suppressor miR-34c targets MET in prostate cancer cells.

Hagman, Zandra; Haflidadottir, Benedikta; Ansari, Mahreen; Persson, Margareta; Bjartell, Anders; Edsjö, Anders; Ceder, Yvonne

Published in:
British Journal of Cancer

DOI:
10.1038/bjc.2013.449

2013

miR-205 negatively regulates the androgen receptor and is associated with adverse outcome of prostate cancer patients

Zandra Hagman[1], Benedikta S. Haflidadóttir[1], Jens A. Ceder[2], Olivia Larne[1], Anders Bjartell[3], Hans Lilja[1,4], Anders Edsjö[5], Yvonne Ceder[1]

[1] Department of Laboratory Medicine, Division of Clinical Chemistry, Lund University, Malmö, Sweden

[2] Department of Clinical Sciences, Division of Urological Research, Lund University, Malmö, Sweden

[3] Department of Clinical Sciences, Division of Urological Cancers, Lund University, Malmö, Sweden

[4] Department of Surgery (Urology), Clinical Laboratories, Epidemiology and Biostatistics, Memorial Sloan-Kettering Cancer Center, New York, NY

[5] Department of Laboratory Medicine, Center for Molecular Pathology, Lund University, Malmö, Sweden

Running title: miR-205 in prostate cancer

To whom correspondence should be addressed:

Dr. Yvonne Ceder, Department of Laboratory Medicine, Malmö, Division of Clinical Chemistry, Wallenberg laboratory, Floor 4, 20502 Malmö, Sweden

Email: Yvonne.Ceder@med.lu.se, Phone: +46 40 338116

Abstract

Background: The microRNA-205 (miR-205) has been shown to be deregulated in prostate cancer. Here we continue to investigate the prognostic and therapeutic potential of this microRNA.

Methods: The expression of miR-205 is measured by qRT-PCR and *in situ* hybridization in a well-documented prostate cancer cohort. An AGO2 based RIP-Chip assay is used to identify targets that are verified with western blots, luciferase reporter assay, ELISA and immunohistochemistry.

Results: The expression of miR-205 is inversely correlated to occurrence of metastases and shortened overall survival, and is lower in castration resistant prostate cancer patients. The miR-205 expression is mainly localized to the basal cells of benign prostate tissues. Genes regulated by miR-205 are enriched in *e.g.* the MAPK/ERK, Toll-like receptor and IL-6 signaling pathways. We demonstrate binding of miR-205 to the 3'UTR of androgen receptor and decrease of both androgen receptor transcript and protein levels. This finding was corroborated in the patient cohort were miR-205 expression inversely correlated to androgen receptor immunostaining in malignant prostate cells and to serum levels of PSA, an androgen regulated protein.

Conclusion: Taken together these findings imply that miR-205 might have therapeutic potential, especially for the castration resistant and currently untreatable form of prostate cancer.

Key words: miRNA, miR-205, prostate cancer, androgen receptor, CRPC, metastases

Introduction

Prostate cancer (PCa) is the most common cancer in men in the developed countries (Jemal *et al*, 2011). Most of these tumors are indolent and curable, but a few are aggressive. The focus of much of today's research is to find markers to determine at an early state which tumors will be life threatening and are in need of radical treatment. Androgen signaling through the androgen receptor (AR) is an important oncogenic pathway for PCa progression. Androgen deprivation therapy is a common treatment modality for advanced disease, but after initial regression of tumor burden, the disease will progress to a castration resistant form (CRPC), for which there currently is no effective cure. Despite the low levels of androgens achieved by the androgen deprivation therapy, increased AR signaling is a key feature of CRPC, through *e.g.* increased expression of the AR, increased sensitivity of the AR to androgens, ligand promiscuity or ligand independent activation of the AR (Feldman & Feldman, 2001). The prostate is composed of a stromal and glandular compartment. The glands of the prostate are predominantly made up of basal epithelial cells and luminal cells. The basal cells are generally undifferentiated and androgen independent, and they have a relatively high proliferative and a low apoptotic rate. The basal cells and progenitor cells continuously adds to the pool of the luminal layer that consists of differentiated cells that secrete various androgen regulated proteins such as prostate specific antigen (PSA).

The human genome encodes around 2000 microRNAs (miRNAs), each of which is capable of regulating hundreds of protein coding genes (Baek *et al*, 2008; Farh *et al*, 2005; Selbach *et al*, 2008; Stark *et al*, 2005). In general miRNAs bind the 3'UTR of mRNAs resulting in a block of translation or degradation of the mRNA (Du & Zamore, 2005; He & Hannon, 2004). However, there have been reports of direct miRNA binding resulting in increased translation of target mRNA (Vasudevan *et al*, 2007). miRNAs have emerged as important regulators of gene expression, and there have been several reports of individual

deregulated miRNAs that have tumor suppressive or oncogenic properties in PCa (Boll *et al*, 2012; Fuse *et al*, 2011; Jalava *et al*, 2012). For example, the expression of miR-205 has been shown to be decreased in PCa, partly explained by hypermethylation of the CpG islands in the *miR-205* promoter, (Bhatnagar *et al*, 2010; Hulf *et al*, 2011; Ke *et al*, 2009; Wiklund *et al*, 2011) and to act as a tumor suppressor by affecting migration, invasion and growth (Boll *et al*, 2012; Gandellini *et al*, 2009; Majid *et al*, 2010; Schaefer *et al*, 2010). However, the mechanisms of action and individual targets has only limited been investigated. In this paper we put our efforts to verify prognostic powers of miR-205 in PCa in a well-documented cohort with a long follow up. The expression of miR-205 has been found to be significantly lower in PCa compared to the BPH samples in this cohort (Larne *et al*, 2012) and receiver operator characteristic curves for differentiation of patients with clinical localized prostate cancer from those with BPH gave an area under the curve of 0.80 (95% CI 0.70 – 0.90). In addition we aim to determine the expression pattern of miR-205 in prostate tissue and identify novel targets of miR-205. These findings will provide new insight into PCa disease biology and could potentially result in novel therapeutic approaches.

Materials and Methods

Tissue specimens and cell culture

The prostate cancer cell lines were obtained from American Type Culture Collection (DU145, PC3, 22Rv1 and LNCaP clone FGC) and European Collection of Cell Cultures (PNT2 and VCaP). The cells were cultured according to the manufacturer's recommendations. The prostate cohort of 49 PCa and 25 patients without PCa has been described previously (Hagman *et al*, 2010). It is to be noted that this is a pre PSA screening era, TURP (transurethral resection of the prostate) cohort. Consequently, the Gleason score/WHO grade is higher and the outcome is worse than in a random contemporary PCa cohort. The patients undergoing treatment at the time of TURP received either testicular ablation or chemical treatment (zoladex, decapeptyl or eulexine). CRPC was defined as biochemical recurrence; two consecutive PSA levels > 0.2 ng/ml or one single observation > 1 ng/ml or clinical progression. The percentage of cancer cells in the samples (5-90%) was determined by a pathologist on the adjacent slide. Detailed information regarding the clinical parameters can be seen in Sup Table 1. Adjacent tissue section slides were used for the immunohistochemistry (IHC) detection of AR and RNA extraction and qRT-PCR of miR-205. For external validation of the correlation between miR-205 and AR transcript levels we analyzed a microarray data set from Taylor *et al*. constituting 110 prostate cancer tissue samples and 28 non-malignant adjacent benign prostate tissue samples (Taylor *et al*, 2010) (GEO accession number GSE21032).

IL-6 concentrations in culture lysate were determined by a commercial enzyme-linked immunosorbent assay (ELISA; cat# 900-K16, Peprotech, Rocky Hill, NJ). Cells were transiently transfected with either miRIDIAN microRNA Mimic (80 nM, Dharmacon, Lafayette, CO) or miRCURY LNA Knockdown probes (100 nM, Exiqon, Denmark) using Oligofectamin reagent (Invitrogen, Carlsbad, CA). Control experiments were performed in

parallel, transfecting cells with miRIDIAN microRNA Mimic Negative Control (Dharmacon) and scramble-miR (Exiqon), respectively.

QRT-PCR

RNA was extracted from the prostate cohort and the different cell lines as described previously (Hagman *et al*, 2010). We also analyzed the expression of miR-205 in different human tissues, with RNA extracted as described previously (Lundwall *et al*, 2002). The miRNA levels were quantified by the TaqMan MicroRNA Assays (Applied Biosystems, Foster City, USA) according to the manufacturer's protocol and as described previously (Hagman *et al*, 2010). For normalizing the expression in the cell lines the geometric mean of RNU48, RNU66 and RNU24 was used. For normalizing the expression of miR-205 in different human tissues the geometric mean of RNU66, RNU48, RNU44 and RNU24 was used.

Androgen receptor expression levels

Total RNA was extracted with Trizol (Invitrogen), according to the manufacturer's protocol. A total of 500 ng RNA was reverse transcribed (random hexamers and Oligo(dT) primers) using the RevertAid™ H Minus First Strand cDNA Synthesis Kit (Fermentas, Thermo Scientific, Germany). The qRT-PCR was performed using specific AR primers (Applied Biosystems, cat. #4331182), and the TaqMan master mix (Applied Biosystems, cat. #4369016).

Androgen regulation

The expression level of miR-205 was determined by qRT-PCR in LNCaP cell lines in the absence or in the presence of androgens. Cells were seeded in normal media and the day after, media was changed to androgen free media with charcoal stripped fetal bovine serum

(Invitrogen). After three days 0, 0.1 or 1 nM R1881 (a synthetic androgen) was added to the medium. Total RNA was extracted two days later with Trizol (Invitrogen). The miR-205 levels were quantified using the TaqMan MicroRNA Assays (Applied Biosystems) as described above. RNU48 was used as endogenous control. As a positive control for the experiment, concentrations of free and total PSA were measured with a dual label immunofluorometric assay (DELFIA Prostatus™ PSAF/T, Perkin-Elmer Life Sciences, Finland) (Mitrunen *et al*, 1995) and concentration of KLK2 was measured as described in previously (Vaisanen *et al*, 2006). Both PSA and KLK2 levels increased with higher concentrations of R1881.

In situ hybridization

In situ hybridization was performed essentially as described previously (Hansson *et al*, 2002), with some modifications. Briefly, formalin fixed paraffin embedded tissues slides were deparaffinized, rehydrated and digested with 10 μg/ml proteinase K (Fermentas) in proteinase K buffer (30 mM Tris-HCl pH 7.5 and 10 mM $CaCl_2$). The slides were refixed with 4% paraformaldehyde (pH ~ 9), and thereafter fixed further with 1-methylimidazol buffer (0.13 M 1-methylimidazol, 300 mM NaCl, pH 8) for 2 x 10 min and EDC (0.16 M 1-ethyl-3(3-dimethylaminopropyl) carbodiimide) for 1 h in a humified chamber. The slides were acetylated and pre-hybridized in hybridization buffer (50% formamide, 5 x SSC, 5 x Denhardt's, 10% dextran, 10% CHAPS, 20% Tween, 0.4 mg/ml salmon sperm DNA, and 20 mg/ml Roche blocking reagent) at the probes Tm minus 23°C for 1h and then O/N at the same temperature with hybridization buffer containing 250 nM locked nucleic acid (LNA) double DIG (3' and 5') antisense probe (Exiqon). The slides were incubated with blocking reagent (TSA kit #T20915, Invitrogen) for 1 h and then with 1:100 anti-DIG-AP antibody (#11093274910, Roche, Germany) for 1 h. Slides were washed, equilibrated in AP buffer

(100 mM Tris-HCl pH9.5, 50 mM $MgCl_2$, 100 mM NaCl) and developed with NBT/BCIP/levamisol solution (75 mg/ml NBT (nitro-blue tetrazolium), 50 mg/ml BCIP (5-bromo-4-chloro-3'-indolyphosphate p-toluidine salt), 0.25 mg/ml levamisol, 0.05% Tween 20, in AP buffer). The reaction was stopped after color development and the slides were mounted with ProLong Gold (P36930, Invitrogen). The specificity of the *in situ* hybridization was determined by a negative scramble double DIG labeled LNA probe (Exiqon) that did not give any signal (Sup. Fig. 1). We also added mimic miRNA probes with 0, 1, 2 or 3 miss-matches to the hybridization buffer, in addition to the DIG-labeled detection probe, in a competition assay. The signal was abolished when adding a surplus of mimic miRNA. The signal increased stepwise by increasing the number of mismatches in the probe (Sup Fig. 1).

In situ hybridization combined with immunohistochemistry

To further characterize the cellular expression pattern of miR-205 in prostatic tissue we used tyramide signal amplification (TSA) and co-detection of cytokeratin 5, a basal cells marker. After hybridization as described above, the slides were immersed in 3% H_2O_2 in PBS for 30 min. The slides were blocked (TSA kit, Invitrogen) for 1 h and then incubated with 1:100 diluted anti-DIG antibody (#11333062910, Roche) for 1 h. The slides were incubated with anti-mouse-HRP antibody (TSA kit) for 1 h and then incubated in the dark with tyramide diluted in amplification buffer (TSA kit) for 10 min. IHC was performed by incubating with an antibody against cytokeratin 5 (Ab776, clone 34bE12, Abcam, UK), diluted 1:500, for 1 h. The slides were washed and incubated with anti-rabbit-alexa (#A11008, Invitrogen, green emission) for 1 h. Finally, the slides were incubated with 4',6-diamidino-2-phenylindole (DAPI, D1306, Invitrogen) for 12 min. The slides were mounted with ProLong Gold (Invitrogen) and photos were taken with Olympus AX70 microscope (filter from Semrock for fluorescence), equipped with a Nikon digital camera.

Immunoprecipitation of human AGO2 complexes in PC3 cells

The immunopurification protocols were adapted from (Easow *et al*, 2007) and (Peritz *et al*, 2006). Cells were trypsinized two days after transfection with miR-205 or scramble mimics, and washed in cold PBS before lysis of the cells (20mM Tris-HCl pH 7.5, 150 mM NaCl, 0.3% Nonidet P-40, 2 mM EDTA, 1mM NaF, 1mM DTT, Protease inhibitor (Pierce), Superase In (Applied Biosystems)). The lysate was kept on ice for 30 min before centrifugation at 10 000 x g for 30 min at 4°C. To reduce background signal, the lysate was pre-cleared with protein G sepharose beads (4 fast flow, GE Healthcare) blocked with 1 mg/ml tRNA (Applied Biosystems) and BSA (1mg/ml, RNase free) for 30 min on rotation at 4°C, before incubated with antibody against human AGO2 (11A9, IgG2a, rat, Ascenion, Germany (Rudel *et al*, 2008)) on rotation O/N at 4°C. The next day the mixture was incubated with blocked protein G sepharose beads on rotation at 4°C for 2 hours. The sample was washed four times with wash buffer (50 mM Tris-HCl pH 7.5, 500 mM NaCl, 0.3% Nonidet P-40, 1 mM $MgCl_2$, Superase In) and one time with PBS. Thereafter the protein/RNA complexes were digested with 40 µg Proteinase K (Qiagen) in 30 mM Tris-HCl pH 8, 10 mM EDTA, 1% SDS buffer, for 30 min at 50°C. The RNA was isolated by phenol/chloroform extraction and EtOH precipitation essentially as described earlier (Chomczynski & Sacchi, 1987). The RNA concentration was measured using a NanoDrop (ND-1000, Spectrophotometer, Thermo Scientific, Wilmington, DE) and the RNA quality assessed using a bioanalyzer (Agilent 2100 Bioanalyzer, Santa Clara, CA).

Microarray hybridization and data analysis

Single stranded cDNA was generated using the GeneChip® Whole Transcript cDNA Synthesis and Amplification Kit (Affymetrix Inc, Santa Clara, CA) using 100 ng of total RNA. Amplified cDNA was fragmented and labeled using the GeneChip® WT Terminal Labelling

Kit (Affymetrix). Subsequently, the biotinylated cDNA was hybridized to the GeneChip® Human Gene 1.0 ST Arrays (Affymetrix). The arrays were washed and stained on a GeneChip® Fluidics Station 450 (Affymetrix) according to the manufacturer's recommendations. Arrays were scanned using the GeneChip® Scanner 3000 and image analysis was performed using GeneChip® Operating Software (Affymetrix), and in Genepix 4.0 (Axon Instruments). The data were normalized, background-corrected, and summarized using the Robust Multichip Average (RMA) algorithm implemented in the Expression Console™ version 1.1.2 software (Affymetrix). The data was analyses using SAM analysis to identify significantly differentially expressed genes between the groups. The list of differentially expressed genes (thresh hold > 1.5; and q = 0) was analyzed using Ingenuity Pathway Analyses (Ingenuity, Montain View, CA). A score was computed for each network according to the fit of the original set of significant genes. This score reflects the negative logarithm of the p-value, which indicated the likelihood of the focus genes in a network being enriched in the data set by chance.

Western blot

Cells were lysed with M-PER (Pierce, Rockford, IL) supplemented with Halt™ protease inhibitor cocktail EDTA-free (Pierce) and 13.4 mM EDTA. Protein concentration was measured and equal amount of proteins were separated on a NuPAGE (Invitrogen) and transferred onto an Immobilon PVDF membrane (Millipore Corporation, Bedford, MA). The membrane was incubated with antibodies directed against E-cadherin 1:2000 (#610181, BD Biosciences), EPCaM 1:100 (sc25308, Santa Cruz Biotechnology, Inc., Santa Cruz, CA), AR 1:100 (N-20, Santa Cruz Biotechnology, Inc.), GAPDH 1:20000 (a-GAPDH, MAB374, Chemicon, CA) and α-actinin (sc-17829, Santa Cruz Biotechnology). Signals from HRP coupled polyclonal secondary antibodies (mouse or rabbit, Dako, Denmark) were generated

by ECL (ECL plus, GE Healthcare) and recorded using a CCD camera (LAS-3000, Fujifilm, Japan). Band intensities were quantified and normalized to GAPDH, using the ImageJ software.

AR 3'UTR construct and luciferase assay

Due to the length of the AR 3'UTR region (almost 7 kb) it has been cloned in several pieces, seven fragments have been described earlier (Ostling *et al*, 2011), but the missing part (fragment 8, located 4344 - 5364 bp upstream of the stop codon in the AR 3'UTR (Ostling *et al*, 2011) was synthesized and cloned into the pMIR-REPORT Luciferase vector (Ambion, Austin, TX) by DNA2.0 (CA, USA). For luciferase assays, PC3 cells were seeded 24 h before transfection. The cells were co-transfected with 1 μg of AR 3′-UTR reported plasmid, 40 ng of Renilla luciferase plasmid and with 80 nM of mimic with Lipofectamine 2000 (Invitrogen). Firefly luciferase and Renilla activity was assayed 48 h after transfection with a Dual-Glo Luciferase Assay System (Promega, WI).

In vitro attachment assay

Three days after PC3 and 22Rv1 cells were transfected, $1 \cdot 10^5$ cells were seeded in a 12 well plate. Five hours later the cells were fixed and stained with sulforhodamine B (SRB), to determine cell density, LNCaP cells were allowed to attached for 24 h. Cells were fixed in 10% trichloroacetic acid and stained with 0.4% SRB (SIGMA-Aldrich, St Louis, MO) in 1% acetic acid for 15 min. Bound SRB was dissolved in 10 mM Tris base and absorbance was read at 490 nm using a microplate reader (El808, BioTek Instruments, Winooski).

Statistical analysis

The real time qRT-PCR data is presented as median and analyzed by the Mann Whitney test. GraphPad Prism version 5 was used for statistical analysis (La Jolla, CA). For *in vitro* assay results we used Student's t-test, where $p < 0.05$ was considered significant.

Results

Expression of miR-205 in a prostate cancer cohort

The prognostic properties of miR-205 expression levels, as measured by qRT-PCR on RNA extracted from FFPE prostatic tissues, were investigated. The clinical characteristics of the cohort have been thoroughly described previously (Hagman *et al*, 2010), but a shorter version can be seen in Sup. Table 1. We found that miR-205 levels were significantly lower in patients with metastases compared to patients without metastasis ($p = 0.004$, Mann-Whitney test), see Fig. 1a. A Kaplan–Meier analysis of patient overall survival based on miR-205 expression levels divided into low (< median) and high (> median) expression, significantly divides the PCa patients into high risk (median survival of 2 years) and low risk patients (median survival of 3 years) ($p = 0.025$, log-rank test), with a hazard ratio of 2.33 (95% CI 1.11 – 4.88), see Fig. 1b. The same result was obtained if only the men that have PSA values from the diagnosis are tested. We found miR-205 level to be highest in BPH and decrease with higher WHO grade, the median miR-205 expression in BPH = 1.67, WHO I = 0.77, WHO II = 1.03, WHO III = 0.64 (Cuzick's trend test $p < 0.0001$). The expression of miR-205 was also measured in six prostate cell lines: 22Rv1, DU145, LNCaP, PC3, VCaP and PNT2. In concordance with the findings in the primary tumor cohort the expression was very low to undetectable in all prostate cancer cell lines, whereas the expression was high in the immortalized normal cell line PNT2 (Sup. Fig. 2).

Expression of miR-205 in the epithelial cells of prostate glands

To determine the histological expression pattern of miR-205 in prostatic tissues, we performed *in situ* hybridization on prostatic tissues from ten patients using double DIG labeled LNA antisense-miR-205. NBT/BCIP detection of miR-205 demonstrated a strong signal in the epithelial cells of the prostate glands, whereas the stromal cells lacked miR-205 expression (Fig. 2a). Consistent with the qRT-PCR results we could see a lower expression of miR-205 in cancer foci. To be able to more specifically verify the cellular location, TSA amplification for detection of miR-205 expression in prostate tissue was performed. This detection method gave the same pattern as with NBT/BCIP detection; cytoplasmic within the epithelial cells. By a combined IHC and *in situ* hybridization assay, to detect expression of the prostate basal marker cytokeratin 5 and miR-205, miR-205 was found to be expressed in the basal cells (Fig. 2b). The expression of miR-205 was also analyzed in different human tissues using qRT-PCR (Sup. Fig. 3). Amongst the tissues with high miR-205 expression was breast, vas deferens, urethra, seminal vesicles, prostate and epididymis; tissues that are regulated by steroid hormones. This suggested that miR-205 might be hormonally regulated. Supporting this notion, *in silico* analyses of the promoter region of the miR-205 gene revealed potential androgen responsive elements. To investigate this LNCaP cells were grown in charcoal stripped media with (0.1 or 1 nM R1881) or without androgen and the expression of miR-205 was measured by qRT-PCR. Expression of miR-205 was detected in androgen depleted conditions, but increased significantly in the presence of R1881. Adding 0.1 nM R1881 gave a 105% increase and adding 1 nM R1881 gave a 139% increase; see Fig. 3, indicating that androgens are not essential, but can incite miR-205 expression.

Regulation of the Androgen Receptor

The miR-205 levels in castration resistant patients (patients that have failed androgen ablation treatment) were found to be significantly lower than in hormone naïve patients ($p = 0.0045$;

Mann-Whitney test), see Fig. 1c. In addition, an inverse correlation between miR-205 levels and pre-TURP total PSA was found (p = 0.019; Spearman test). Since PSA is regulated by androgens through the AR, and castration resistance often is linked to increased AR levels, these findings raised the question whether miR-205 might be involved in regulation of the AR. To investigate this we made *in vitro* expression studies. Ectopic expression of miR-205 resulted in decreased AR transcript levels in 22Rv1 (62% decrease, p = 0.018) and in LNCaP cells (40% decrease, p = 0.034), see Fig. 4a. In concordance with this, ectopic expression of miR-205 also resulted in a decrease of AR protein levels in VCaP (80% decrease, p = 0.015) and 22Rv1 (38% decrease, p = 0.018), see Fig. 4b. In the LNCaP cells the result was spread and although there was a trend (27% less AR proteins four days after transfection, and 37% less five days after transfection) this was not statistically significant (results not shown). Using the target prediction program RNA22, we found miR-205 binding site in the AR 3'UTR, both in fragment 2, 4 and 8. This was tested by luciferase reporter assays in the AR negative cell line to avoid binding to the endogenous protein. Vectors containing fragment 1 – 8 of the AR 3'UTR were co-transfected with miR-205 or scramble mimics. A significant reduction in luciferase signal was seen for construct 8 in PC3 (p = 0.005), indicating that miR-205 can regulate the AR expression level by binding to this part of the 3'UTR. Further, blocking endogenous levels of miR-205 in PNT2 (the only cell line with high miR-205 levels as shown in Sup. Fig. 2) gave an increased binding of miR-205 to construct 8 of the AR 3'UTR, indicating that this interaction can occur in prostate cells. Next we analyzed whether miR-205 inversely correlate with AR levels in PCa patients. The AR content has previously been determined by IHC on PCa tissue in the investigated cohort (Ostling *et al*, 2011), and we now correlated this to miR-205 expression levels as measured by qRT-PCR on adjacent slides. We found a statistically significant inverse correlation in the malignant epithelial cells (p = 0.023 for intensity score 1 + 2 versus 3; Mann–Whitney test), but no correlation in the benign

epithelium, see Fig. 5. We confirmed an inverse correlation of AR and miR-205 level in an external microarray data set of 138 men ($p = 0.0009$, Spearman, $r = -0.2788$) (Taylor *et al*, 2010).

Identification of potential miR-205 targets in PC3 cells

To further investigate what proteins are directly regulated by miR-205, a RIP-Chip assay was performed, and the enriched mRNAs was analyzed by an Affymetrix microarray. The complete set of targets identified is provided in Sup. Table 2, and the data have been deposited in NCBI's Gene Expression Omnibus (Edgar *et al*, 2002), accession number GSE39735. Pathways in which the identified targets are enriched in were identified by Ingenuity Pathway Analysis, and pathways that are important in cancer came out at the top; *e.g.* the MAPK/ERK, Toll-like receptor and IL-6 signaling pathways (Sup. Table 3). We confirmed an effect on IL-6 levels by ELISA after overexpressing miR-205 (in 22Rv1 a 63% decrease, $p = 0.044$; in LNCaP a 74% decrease $p = 0.008$), see Fig. 6a. We also identified interesting individual miR-205 targets with relevance for tumor progression *e.g.* EGR1, EPCaM, CCL20, FGFBP1, CDH1, FOSB and JUNB, see Table 1. We could confirm an increased level of EPCaM upon miR-205 expression in LNCaP and PC3 cells (Fig. 6b). We also confirmed increased levels of E-cadherin (CDH1) upon miR-205 ectopic expression in PC3 and 22Rv1 cells, in accordance with previous studies done in the androgen independent cell lines DU145 and PC3 cells (Gandellini *et al*, 2009) and in non-prostatic tissues (Gregory *et al*, 2008; Wiklund *et al*, 2011), see Fig. 6c. Interestingly, we did not see this effect in the androgen dependent LNCaP cells. We also found individual targets known to enhance the expression of AR, *e.g.* IL-8 (fold change 3.7) and EDN1 (fold change 3.5); and targets known to inhibit AR, such as ATF3 (fold change 2.3). Furthermore, other members of the nuclear receptor family (NR4A1, NR4A2, and NR4A3) were amongst the miR-205 target.

miR-205 affects adhesion of prostate cancer cells

miR-205 has previously been reported to affect cell proliferation, apoptosis, colony formation, migration and invasion of PCa cells (Gandellini *et al*, 2009; Majid *et al*, 2010). We assessed the effect of miR-205 on cell adhesion using a gain-of-function approach. Ectopic expression of miR-205 in androgen independent PC3 and 22Rv1 cells gave a 103% and 47% increase in adhesion respectively ($p = 0.003$ resp. $p = 0.001$). Transfection of androgen dependent LNCaP cells on the contrary, resulted in 73% less adhesion compared to negative control transfected cells ($p = 0.0004$), see Fig. 7. Ectopic expression of miR-205 or blocking of miR-205 did not affect adhesion in PNT2 (results not shown).

Discussion

In the present study, we examined the expression pattern and potential targets of miR-205 in PCa. We and others have seen that miR-205 is significantly downregulated in PCa specimens and the same was found to be true in prostatic cancer cell lines consistent with previous reports (Gandellini *et al*, 2009; Majid *et al*, 2010; Porkka *et al*, 2007; Schaefer *et al*, 2010). Furthermore, miR-205 expression was higher in patients with localized disease compared to patients with distant metastases, confirming earlier results (Gandellini *et al*, 2009; Tucci *et al*, 2012). Overall survival was one year longer in the group with high levels of miR-205. Furthermore, the expression of miR-205 was found to be localized to the basal cells of the prostate, in agreement with a report published while this paper was prepared (Gandellini *et al*, 2012).

Transient expression of miR-205 was found to affect the levels of AR in androgen dependent VCaP and 22Rv1 cells. We have data indicating binding to the AR 3'UTR by a luciferase assay, both when overexpressing ectopic miR-205 in PC3 and when blocking endogenous levels in PNT2. In LNCaP there is an effect on mRNA level, but no statistically

significant effect on protein levels, although there is a trend. The lack of difference on AR protein level in LNCaP is in accordance with an earlier report (Boll *et al*, 2012). Potentially, miR-205 has other targets in LNCaP that repress AR protein levels and thereby counteract the effect of miR-205 on AR protein levels. One possibility is degradation of phosphorylated AR by the PI3K–AKT pathway (Lin *et al*, 2002), which is induced by growth factors such as PDGFA/B and executed via growth factor receptors such as IGF1R, these are proteins that was present in the IP from LNCaP cells (Boll *et al*, 2012), but not in the PC3 cells.

In the PCa patient cohort, the expression of miR-205 was found to be inversely correlated to AR. This was also verified at transcript level in an external prostate cancer cohort (Taylor *et al*, 2010). In addition, we found that the level of miR-205 inversely correlated to serum levels of the androgen regulated PSA in our cohort, corroborating the targeting of AR signaling. Moreover, miR-205 was lower in castration resistant patients where AR is frequently upregulated (Feldman & Feldman, 2001), compared to hormone naïve patients. It has been observed that many miRNAs and their targets are expressed in a mutually exclusive manner, either temporally or spatially (Stark *et al*, 2005). Targets are typically present in foci adjacent to the miRNA expressing cells. We found that miR-205 is expressed mainly in the basal cells of prostatic glands. The AR expression is mainly localized to the luminal cells, and we did not detect AR in the basal cells, in concordance with earlier results showing that AR expression is undetectable (Prins *et al*, 1991; Uzgare *et al*, 2004) or very low (Bonkhoff *et al*, 1998) in basal cells. In the RIP-Chip assay, miR-205 was found to target pathways important for cancer progression, *e.g.* the IL-6 signaling that was verified in two PCa cell lines. There were also several previously reported miR-205 targets from other tissues identified by the RIP-Chip assay, such as PKP3, IL6, CDH3, EDN1, and FOS (Gandellini *et al*, 2009) (Table S5); IL-24 (Majid *et al*, 2010); CYR61 (Xie *et al*, 2012); EGR1 and IL-18 (Greene *et al*, 2010) (Table S1). However, when comparing our data from PC3 cells to a similar RIP-Chip assay

performed in LNCaP cells (Boll *et al*, 2012) the results are very different. Only 4% of the miR-205 targets (with a thresh hold of > 1.5 fold) we found in PC3 cells overlapped with the miR-205 targets reported in LNCaP (Boll *et al*, 2012). The discrepancy could be due to differences in methodology, the available transcriptomes (*e.g.* the androgen regulated KLK2 identified in the LNCaP cells is not expressed in PC3 cells) or target sequences variations, but also that miR-205 might be acting by other mechanisms in an androgen independent setting compared to an androgen dependent. It is possible that cofactors essential for miR-205 action are repressed by androgen signaling. This hypothesis is strengthen by a resent paper that show that miR-205 negatively affect viability only in the absence of androgen (Hulf *et al*, 2012). This is an interesting concept since the natural setting of miR-205 is in the AR-devoid basal cells, hence the augmenting effect of androgens on miR-205 expression could be counteracted in AR containing cells by an alternative mechanism ensuring that miR-205 action is not occurring outside the original site of expression. This would imply that if endogenous miR-205 was used therapeutically, it would decrease the AR in the androgen independent malignant epithelial, luminar and possibly stem cells, but without affecting the benign epithelial cells. As we continued to investigate other targets of miR-205, we found more examples of differential regulation in the androgen dependent and independent cell lines. Ectopic expression of miR-205 increases E-cadherin protein levels in 22Rv1 and PC3 cells (also seen in DU145 (Gandellini *et al*, 2009)), but not in LNCaP cells. We also find differences between the androgen dependent and independent cell lines when studying adhesion. Ectopic expression of miR-205 induces increased adhesion in PC3 and 22RV1 cells, but decreased adhesion in LNCaP cells (in PNT2 adhesion was not affected by miR-205). These results indicate that a decrease of miR-205 in PCa would give less adhesion in an androgen independent setting, with concomitant increase in migration and invasion. This

could possibly accounts for parts of the increased risk of metastasis that was seen in the patient cohort.

One of the few pathways that were affected by miR-205 both in PC3 and LNCaP cells was the MAPK pathway, however targeting different transcripts in the pathway. MAPK signaling is involved in AR phosphorylation which has been suggested to increase the ligand-independent activation of the AR under low androgen conditions such as castration. The MAPK pathway is also an oncogenic pathway that can promote growth and survival.

In conclusion, we find that miR-205 is correlated to overall survival and inversely correlated with negative prognostic parameters such as occurrence of distant metastases and castration resistance. This could be explained by the cellular location of miR-205 and the androgen influenced effects on individual oncogenes and oncogenic pathways. These findings might have therapeutic implications especially for the castration resistant and currently untreatable form of prostate cancer.

Acknowledgement

We thank Elise Nilsson for preparing prostatic tissue samples and Margareta Persson for technical assistance. AR 3'UTR constructs was a kind gift from Päivi Östling (Medical Biotechnology, VTT Technical Research Centre of Finland, and Turku Centre for Biotechnology, University of Turku and Åbo Akademi University, Turku, Finland). The research leading to these results has received funding from the European Union Seventh Framework Programme (*FP7/2007-2013*) under *grant agreement* n°*201438*, the Swedish Research council, Gunnar Nilssons Cancer foundation, Jeanssons foundation and Gyllenstiernska Krapperups foundation. The authors disclose no potential conflicts of interest.

References

Baek D, Villen J, Shin C, Camargo FD, Gygi SP, Bartel DP (2008) The impact of microRNAs on protein output. *Nature* **455:** 64-71

Bhatnagar N, Li X, Padi SK, Zhang Q, Tang MS, Guo B (2010) Downregulation of miR-205 and miR-31 confers resistance to chemotherapy-induced apoptosis in prostate cancer cells. *Cell Death Dis* **1:** e105

Boll K, Reiche K, Kasack K, Morbt N, Kretzschmar AK, Tomm JM, Verhaegh G, Schalken J, von Bergen M, Horn F, Hackermuller J (2012) MiR-130a, miR-203 and miR-205 jointly repress key oncogenic pathways and are downregulated in prostate carcinoma. *Oncogene*

Bonkhoff H, Fixemer T, Remberger K (1998) Relation between Bcl-2, cell proliferation, and the androgen receptor status in prostate tissue and precursors of prostate cancer. *Prostate* **34:** 251-8

Chomczynski P, Sacchi N (1987) Single-step method of RNA isolation by acid guanidinium thiocyanate-phenol-chloroform extraction. *Anal Biochem* **162:** 156-9

Du T, Zamore PD (2005) microPrimer: the biogenesis and function of microRNA. *Development* **132:** 4645-52

Easow G, Teleman AA, Cohen SM (2007) Isolation of microRNA targets by miRNP immunopurification. *RNA* **13:** 1198-204

Edgar R, Domrachev M, Lash AE (2002) Gene Expression Omnibus: NCBI gene expression and hybridization array data repository. *Nucleic Acids Res* **30:** 207-10

Farh KK, Grimson A, Jan C, Lewis BP, Johnston WK, Lim LP, Burge CB, Bartel DP (2005) The Widespread Impact of Mammalian MicroRNAs on mRNA Repression and Evolution. *Science* **310:** 1817-21

Feldman BJ, Feldman D (2001) The development of androgen-independent prostate cancer. *Nat Rev Cancer* **1:** 34-45

Fuse M, Nohata N, Kojima S, Sakamoto S, Chiyomaru T, Kawakami K, Enokida H, Nakagawa M, Naya Y, Ichikawa T, Seki N (2011) Restoration of miR-145 expression suppresses cell proliferation, migration and invasion in prostate cancer by targeting FSCN1. *Int J Oncol* **38:** 1093-101

Gandellini P, Folini M, Longoni N, Pennati M, Binda M, Colecchia M, Salvioni R, Supino R, Moretti R, Limonta P, Valdagni R, Daidone MG, Zaffaroni N (2009) miR-205 Exerts tumor-suppressive functions in human prostate through down-regulation of protein kinase Cepsilon. *Cancer Res* **69:** 2287-95

Gandellini P, Profumo V, Casamichele A, Fenderico N, Borrelli S, Petrovich G, Santilli G, Callari M, Colecchia M, Pozzi S, De Cesare M, Folini M, Valdagni R, Mantovani R, Zaffaroni N (2012) miR-205 regulates basement membrane deposition in human prostate: implications for cancer development. *Cell Death Differ*

Greene SB, Gunaratne PH, Hammond SM, Rosen JM (2010) A putative role for microRNA-205 in mammary epithelial cell progenitors. *J Cell Sci* **123:** 606-18

Gregory PA, Bert AG, Paterson EL, Barry SC, Tsykin A, Farshid G, Vadas MA, Khew-Goodall Y, Goodall GJ (2008) The miR-200 family and miR-205 regulate epithelial to mesenchymal transition by targeting ZEB1 and SIP1. *Nat Cell Biol* **10:** 593-601

Hagman Z, Larne O, Edsjo A, Bjartell A, Ehrnstrom RA, Ulmert D, Lilja H, Ceder Y (2010) miR-34c is downregulated in prostate cancer and exerts tumor suppressive functions. *Int J Cancer* **127:** 2768-76

Hansson J, Bjartell A, Gadaleanu V, Dizeyi N, Abrahamsson PA (2002) Expression of somatostatin receptor subtypes 2 and 4 in human benign prostatic hyperplasia and prostatic cancer. *Prostate* **53:** 50-9

He L, Hannon GJ (2004) MicroRNAs: small RNAs with a big role in gene regulation. *Nat Rev Genet* **5:** 522-31

Hulf T, Sibbritt T, Wiklund ED, Bert S, Strbenac D, Statham AL, Robinson MD, Clark SJ (2011) Discovery pipeline for epigenetically deregulated miRNAs in cancer: integration of primary miRNA transcription. *BMC Genomics* **12:** 54

Hulf T, Sibbritt T, Wiklund ED, Patterson K, Song JZ, Stirzaker C, Qu W, Nair S, Horvath LG, Armstrong NJ, Kench JG, Sutherland RL, Clark SJ (2012) Epigenetic-induced repression of microRNA-205 is associated with MED1 activation and a poorer prognosis in localized prostate cancer. *Oncogene*

Jalava SE, Urbanucci A, Latonen L, Waltering KK, Sahu B, Janne OA, Seppala J, Lahdesmaki H, Tammela TL, Visakorpi T (2012) Androgen-regulated miR-32 targets BTG2 and is overexpressed in castration-resistant prostate cancer. *Oncogene*

Jemal A, Bray F, Center MM, Ferlay J, Ward E, Forman D (2011) Global cancer statistics. *CA Cancer J Clin* **61:** 69-90

Ke XS, Qu Y, Rostad K, Li WC, Lin B, Halvorsen OJ, Haukaas SA, Jonassen I, Petersen K, Goldfinger N, Rotter V, Akslen LA, Oyan AM, Kalland KH (2009) Genome-wide profiling of histone h3 lysine 4 and lysine 27 trimethylation reveals an epigenetic signature in prostate carcinogenesis. *PLoS One* **4:** e4687

Larne O, Martens-Uzunova E, Hagman Z, Edsjo A, Lippolis G, Vredenbregt-van den Berg MS, Bjartell A, Jenster G, Ceder Y (2012) miQ - a novel microRNA based diagnostic and prognostic tool for prostate cancer. *Int J Cancer*

Lin HK, Wang L, Hu YC, Altuwaijri S, Chang C (2002) Phosphorylation-dependent ubiquitylation and degradation of androgen receptor by Akt require Mdm2 E3 ligase. *EMBO J* **21:** 4037-48

Lundwall A, Bjartell A, Olsson AY, Malm J (2002) Semenogelin I and II, the predominant human seminal plasma proteins, are also expressed in non-genital tissues. *Mol Hum Reprod* **8:** 805-10

Majid S, Dar AA, Saini S, Yamamura S, Hirata H, Tanaka Y, Deng G, Dahiya R (2010) MicroRNA-205-directed transcriptional activation of tumor suppressor genes in prostate cancer. *Cancer* **116:** 5637-49

Mitrunen K, Pettersson K, Piironen T, Bjork T, Lilja H, Lovgren T (1995) Dual-label one-step immunoassay for simultaneous measurement of free and total prostate-specific antigen concentrations and ratios in serum. *Clin Chem* **41:** 1115-20

Ostling P, Leivonen SK, Aakula A, Kohonen P, Makela R, Hagman Z, Edsjo A, Kangaspeska S, Edgren H, Nicorici D, Bjartell A, Ceder Y, Perala M, Kallioniemi O (2011) Systematic analysis of microRNAs targeting the androgen receptor in prostate cancer cells. *Cancer Res* **71:** 1956-67

Peritz T, Zeng F, Kannanayakal TJ, Kilk K, Eiriksdottir E, Langel U, Eberwine J (2006) Immunoprecipitation of mRNA-protein complexes. *Nat Protoc* **1:** 577-80

Porkka KP, Pfeiffer MJ, Waltering KK, Vessella RL, Tammela TL, Visakorpi T (2007) MicroRNA expression profiling in prostate cancer. *Cancer Res* **67:** 6130-5

Prins GS, Birch L, Greene GL (1991) Androgen receptor localization in different cell types of the adult rat prostate. *Endocrinology* **129:** 3187-99

Rudel S, Flatley A, Weinmann L, Kremmer E, Meister G (2008) A multifunctional human Argonaute2-specific monoclonal antibody. *RNA* **14:** 1244-53

Schaefer A, Jung M, Mollenkopf HJ, Wagner I, Stephan C, Jentzmik F, Miller K, Lein M, Kristiansen G, Jung K (2010) Diagnostic and prognostic implications of microRNA profiling in prostate carcinoma. *Int J Cancer* **126:** 1166-76

Selbach M, Schwanhausser B, Thierfelder N, Fang Z, Khanin R, Rajewsky N (2008) Widespread changes in protein synthesis induced by microRNAs. *Nature* **455:** 58-63

Stark A, Brennecke J, Bushati N, Russell RB, Cohen SM (2005) Animal MicroRNAs confer robustness to gene expression and have a significant impact on 3'UTR evolution. *Cell* **123:** 1133-46

Taylor BS, Schultz N, Hieronymus H, Gopalan A, Xiao Y, Carver BS, Arora VK, Kaushik P, Cerami E, Reva B, Antipin Y, Mitsiades N, Landers T, Dolgalev I, Major JE, Wilson M, Socci ND, Lash AE, Heguy A, Eastham JA, Scher HI, Reuter VE, Scardino PT, Sander C, Sawyers CL, Gerald WL (2010) Integrative genomic profiling of human prostate cancer. *Cancer Cell* **18:** 11-22

Tucci P, Agostini M, Grespi F, Markert EK, Terrinoni A, Vousden KH, Muller PA, Dotsch V, Kehrloesser S, Sayan BS, Giaccone G, Lowe SW, Takahashi N, Vandenabeele P, Knight RA, Levine AJ, Melino G (2012) Loss of p63 and its microRNA-205 target results in enhanced cell migration and metastasis in prostate cancer. *Proc Natl Acad Sci U S A* **109:** 15312-7

Uzgare AR, Xu Y, Isaacs JT (2004) In vitro culturing and characteristics of transit amplifying epithelial cells from human prostate tissue. *J Cell Biochem* **91:** 196-205

Vaisanen V, Peltola MT, Lilja H, Nurmi M, Pettersson K (2006) Intact free prostate-specific antigen and free and total human glandular kallikrein 2. Elimination of assay interference by enzymatic digestion of antibodies to F(ab')2 fragments. *Anal Chem* **78:** 7809-15

Vasudevan S, Tong Y, Steitz JA (2007) Switching from repression to activation: microRNAs can up-regulate translation. *Science* **318:** 1931-4

Wiklund ED, Bramsen JB, Hulf T, Dyrskjot L, Ramanathan R, Hansen TB, Villadsen SB, Gao S, Ostenfeld MS, Borre M, Peter ME, Orntoft TF, Kjems J, Clark SJ (2011) Coordinated epigenetic repression of the miR-200 family and miR-205 in invasive bladder cancer. *Int J Cancer* **128:** 1327-34

Figure legends

Figure 1.

(A) The miR-205 levels in prostate cancer patients with metastasis (denoted 1, n = 18) and without metastases (denoted 0, n = 17). (B) Kaplan–Meier analysis of patient survival based on miR-205 expression levels divided into low (< median) and high (> median) expression. (C) The miR-205 levels in benign hyperplasia (n = 25), hormone naïve (n = 22) and castration resistant prostate cancer (failed androgen ablation treatment) (n= 14).

Figure 2.

(A) *In situ* hybridization with double DIG labeled LNA probe and NBT/BCIP detection. Expression of miR-205 was detected in the epithelial cells in non-cancerous prostate tissue, but not in prostate cancer foci. No signal was seen for negative control in non-cancerous prostate tissue. (B) *In situ* hybridization with double DIG labeled LNA probe and tyramide signal amplification (miR-205, red), was combined with immunohistochemistry on the same tissue section for the basal cell marker cytokeratin 5 (green). The hybridization signals for miR-205 and cytokeratin 5 co-localized suggesting that miR-205 is expressed in the basal cells in non-cancerous prostate tissue. We used DAPI for nuclear staining (blue). Scale bar = 20 μm.

Figure 3.

The expression level of miR-205 increases with increasing androgen concentrations (0, 0.1 or 1 nM R1881). The expression of miR-205 was determined by real-time PCR and the expression of RNU48 was used as an endogenous control.

Figure 4.

(A) AR transcript levels, as measured by qRT-PCR, after ectopic expression of miR-205 in 22Rv1 and LNCaP cells. PGK1 and HPRT1 transcripts were used as endogenous controls. (B) Western blot on the protein levels of androgen receptor (AR) after ectopically expressing miR-205 in VCaP, 22Rv1, and LNCaP cells. GAPDH is used as a loading control. (C) Luciferase reporter assay of AR 3'UTR construct 8. PC3 cells were co-transfected with reporter construct and miRNA mimics. (D) Luciferase reporter assay of AR 3'UTR construct 8. PNT2 cells were co-transfected with reporter construct and LNA antisense. The luciferase signal was measured 24 h after transfection and the firefly luciferase was normalized to Renilla.

Figure 5.

Inverse correlation of miR-205 and AR levels in prostate malignant epithelium. miR-205 was detected with qRT-PCR in 47 prostatic cancer tissues obtained by TURP. The AR protein content in malignant epithelium was determined by immunostaining and scored by overall intensity (score: 1 weak; 2 moderate to strong; and 3 intense). Significant inverse correlation was observed for miR-205 when compared with AR intensity score 1 + 2 versus 3 (Mann–Whitney test).

Figure 6.

(A) The effect of miR-205 on the levels of IL-6 levels in LNCaP and 22Rv1 cells. (B) Western blot on the levels of EPCaM after ectopically expressing miR-205 in 22Rv1 and PC3 cells. (C) Western blot on the levels of E-cadherin after ectopically expressing miR-205 in PC3, 22Rv1, and LNCaP cells. GAPDH or α-actinin was used as loading controls.

Figure 7.

The effect of miR-205 ectopic expression on the attachment potential of PC3, 22Rv1, and LNCaP cells, as measured by a sulforhodamine B assay.

Table 1

Molecules identified by RIP-CHiP, fold change in miR-205 expressing cells compared to control cells.

Supplementary figure 1.

In situ hybridization with double DIG labeled LNA probe and NBT/BCIP detection. Expression of miR-205 was detected in the epithelial cells in non-cancerous prostate tissue. The expression of miR-205 was not detected if a surplus of miR-205 mimic was added. When one mutation was present in the surplus mimic the signal came back, and with two and three mutations the signal increased further.

Supplementary figure 2.

The distribution of miR-205 in six prostate cell lines was determined by real-time PCR. The miRNA levels are presented as the ratio of miR-205 to the geometrical mean of three endogenous controls (RNU48, RNU66 and RNU24).

Supplementary figure 3.

The distribution of miR-205 in 27 different human tissues was determined by real-time PCR. The miRNA levels are presented as the ratio of miR-205 to the geometrical mean of four endogenous controls (RNU48, RNU66, RNU24 and RNU44).

Supplementary table 1.

Clinical characteristics of the prostate cancer cohort.

Supplementary table 2.

List of miR-205 targets from Ago2-IP, identified via microarray analysis.

Supplementary table 3.

Enriched Biofunctions of miR-205 targets identified by RIP-Chip analyses (IPA).

Figure 1

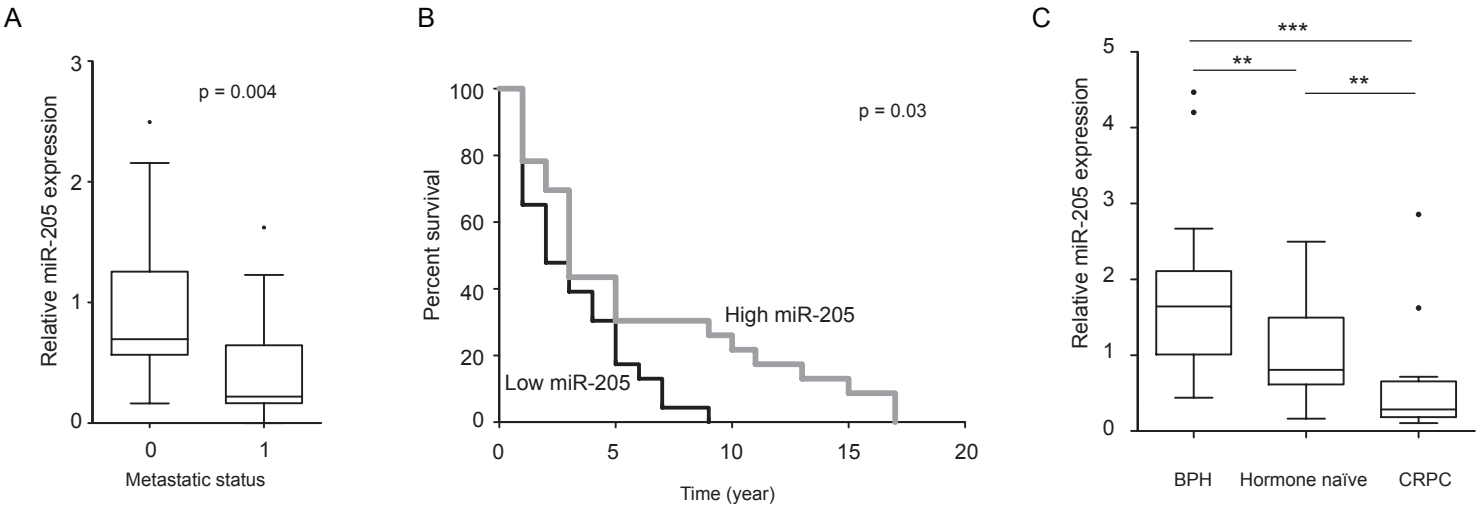
A
Relative miR-205 expression
p = 0.004
Metastatic status
B
Percent survival
p = 0.03
High miR-205
Low miR-205
Time (year)
C
Relative miR-205 expression
***
**
**
BPH
Hormone naïve
CRPC

Figure 2

A

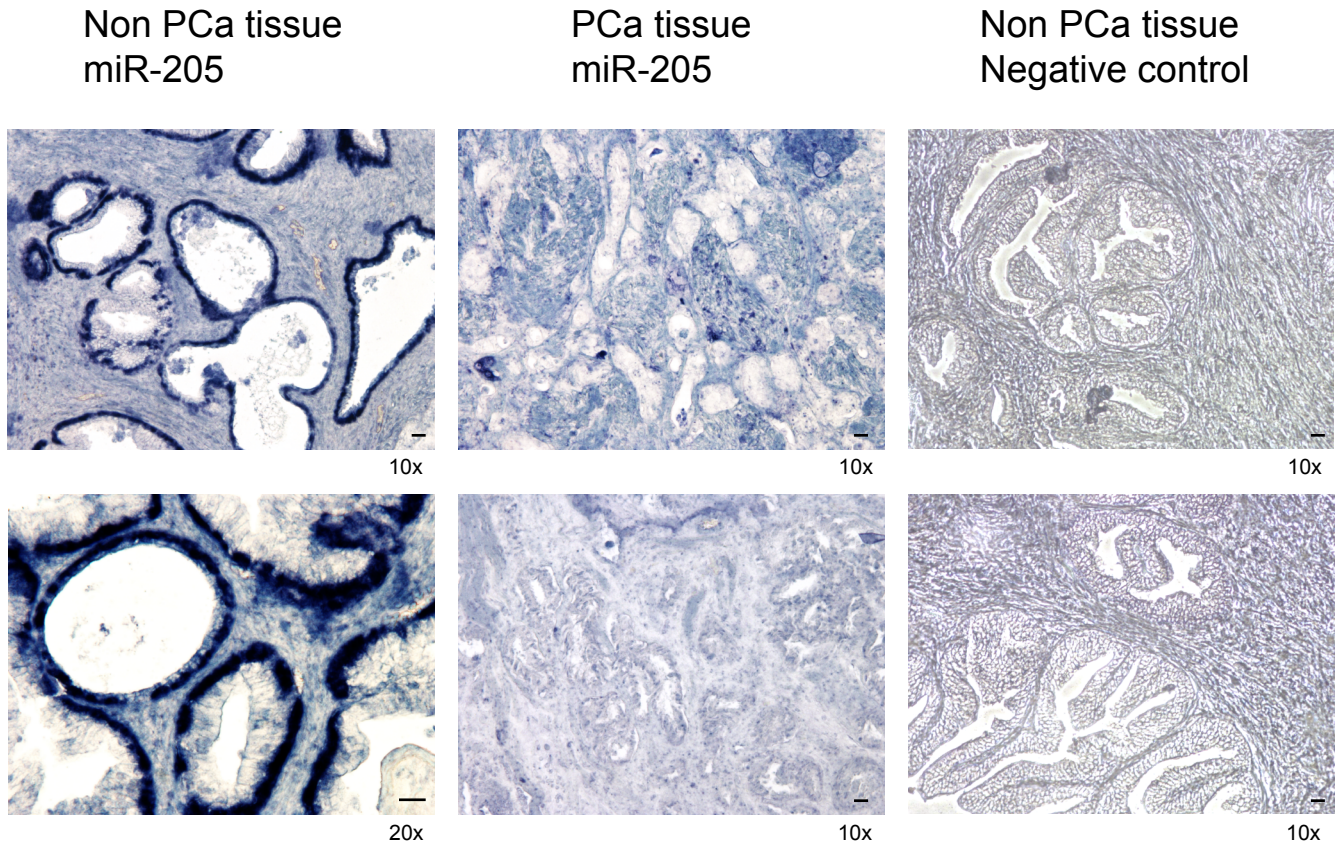
Non PCa tissue
miR-205
PCa tissue
miR-205
Non PCa tissue
Negative control
10x
10x
10x
20x
10x
10x

B

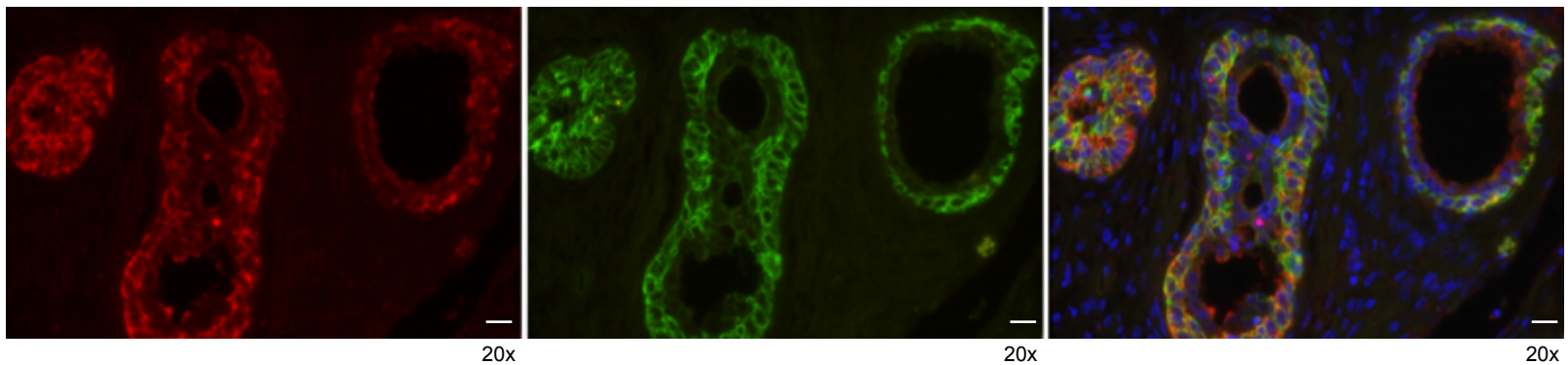
20x
20x
20x
miR-205
Cytokeratin 5
Merged

Figure 3

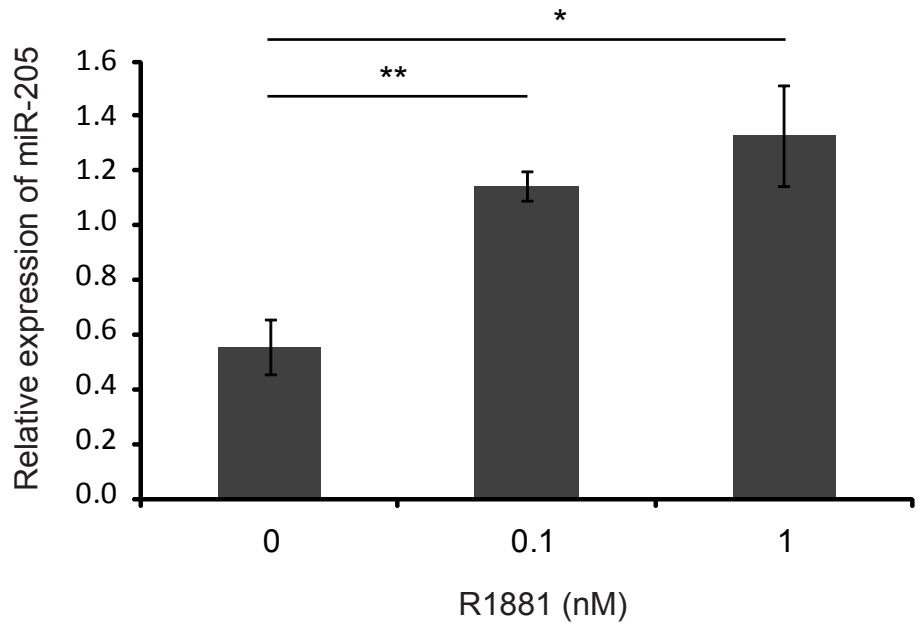
*
**
Relative expression of miR-205
1.6
1.4
1.2
1.0
0.8
0.6
0.4
0.2
0.0
0
0.1
1
R1881 (nM)

Figure 4

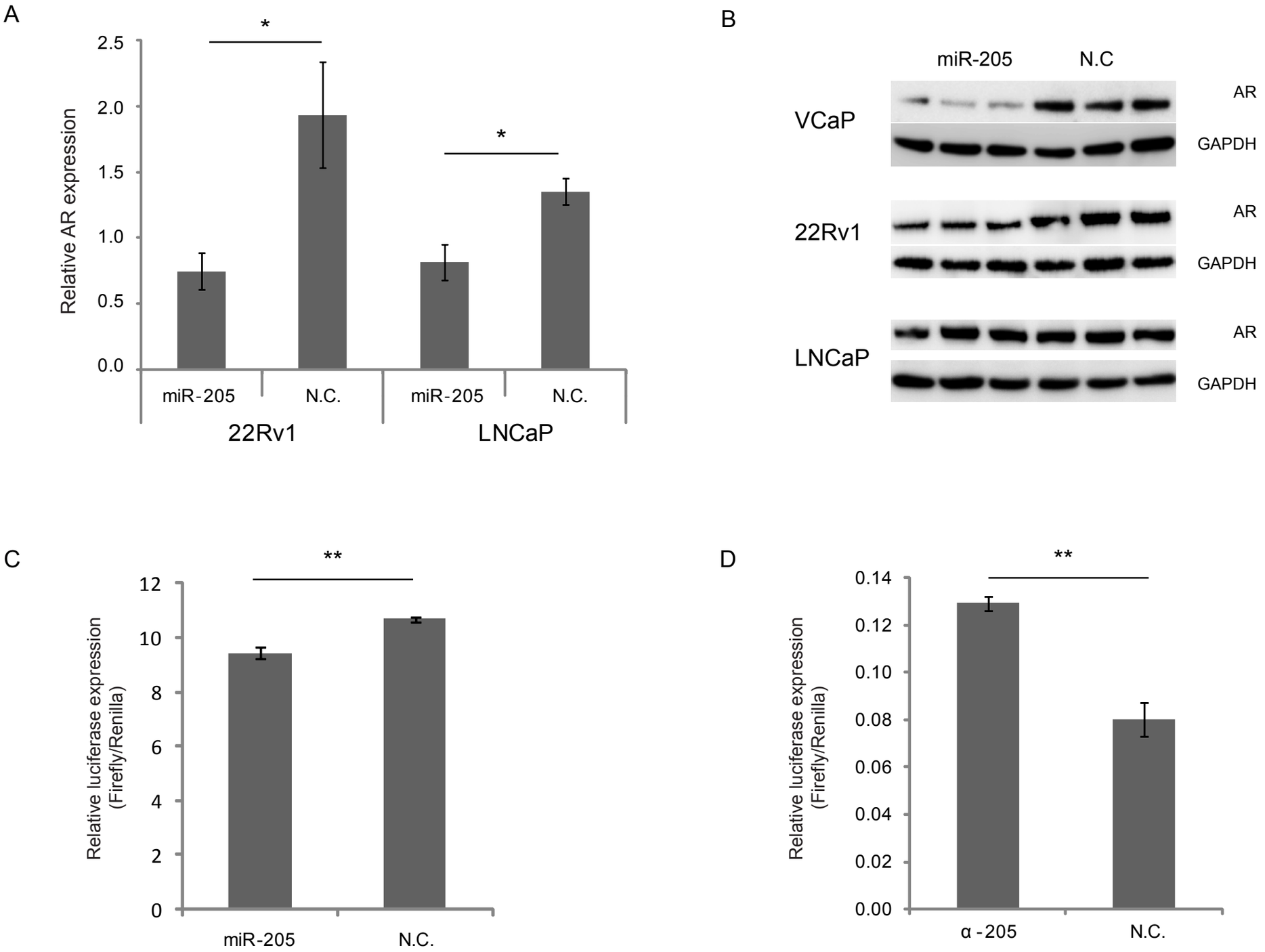
A
*
*
2.5
2.0
1.5
1.0
0.5
0.0
Relative AR expression
miR-205
N.C.
miR-205
N.C.
22Rv1
LNCaP
B
miR-205
N.C
VCaP
22Rv1
LNCaP
AR
GAPDH
AR
GAPDH
AR
GAPDH
C
**
12
10
8
6
4
2
0
Relative luciferase expression (Firefly/Renilla)
miR-205
N.C.
D
**
0.14
0.12
0.10
0.08
0.06
0.04
0.02
0.00
Relative luciferase expression (Firefly/Renilla)
α -205
N.C.

Figure 5

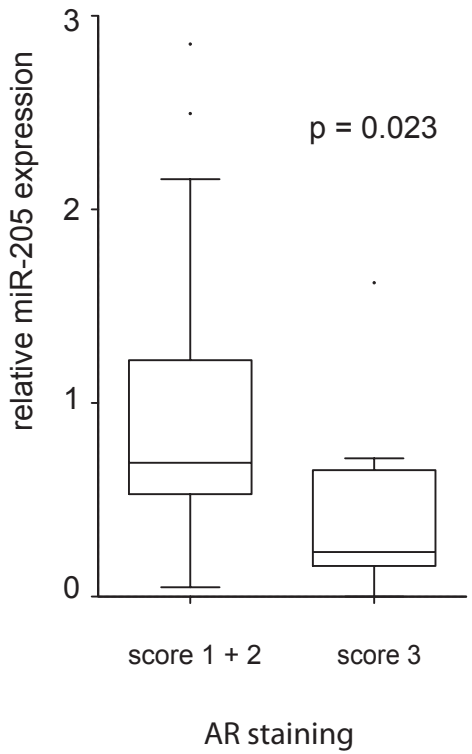
3
2
1
0
relative miR-205 expression
p = 0.023
score 1 + 2
score 3
AR staining

Figure 6

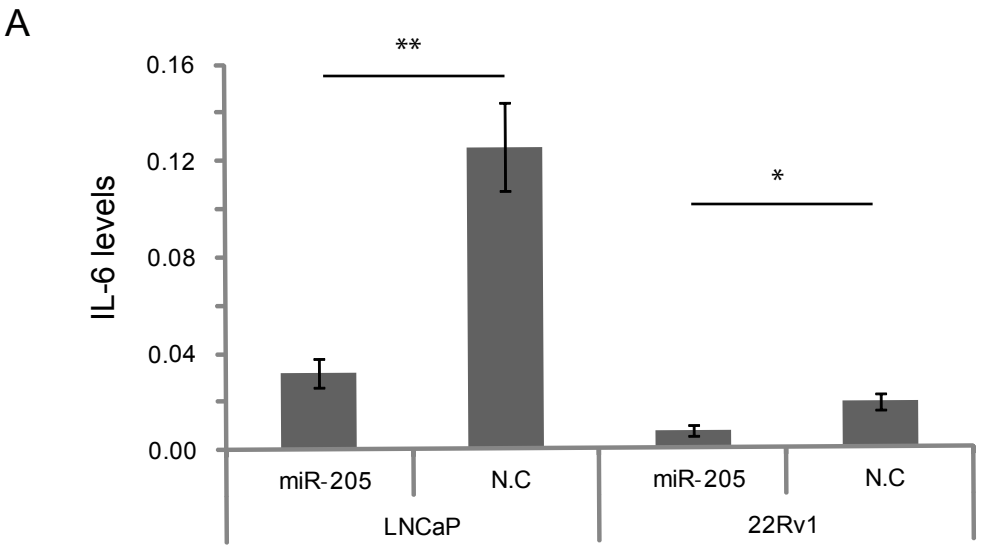
A
**
*
0.16
0.12
0.08
0.04
0.00
IL-6 levels
miR-205
N.C
miR-205
N.C
LNCaP
22Rv1

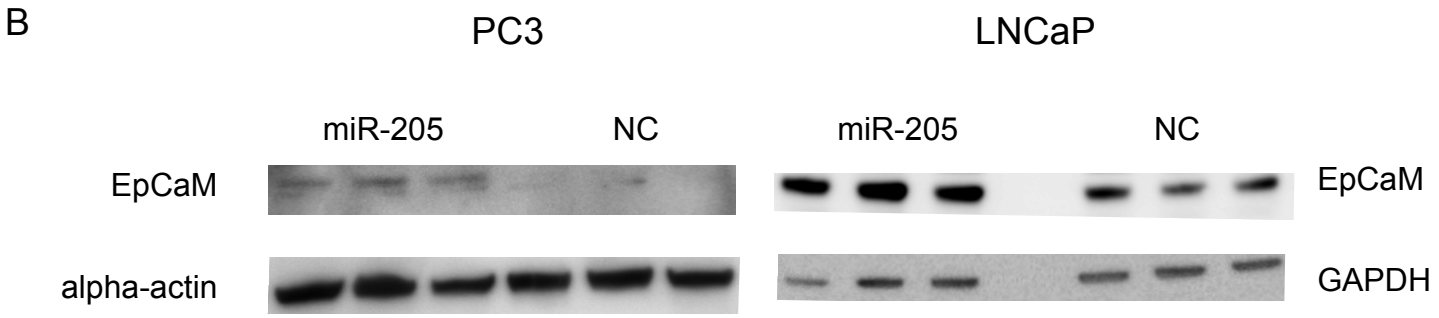
B
PC3
LNCaP
miR-205
NC
miR-205
NC
EpCaM
alpha-actin
EpCaM
GAPDH

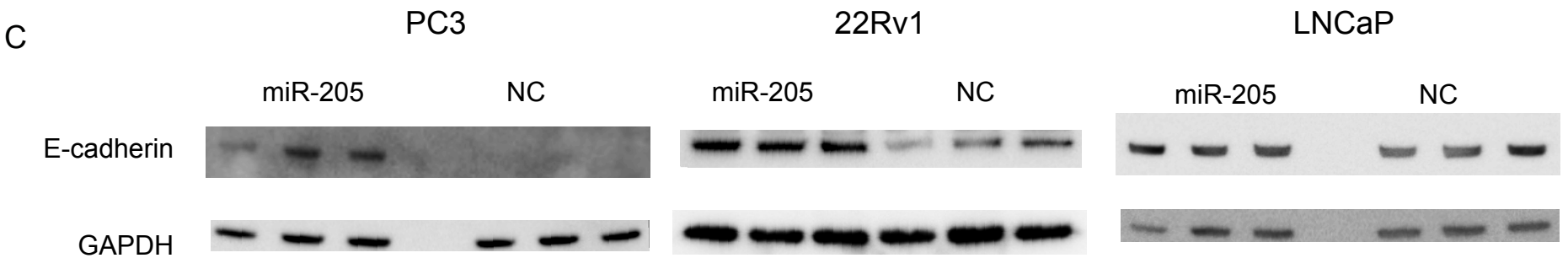
C
PC3
22Rv1
LNCaP
miR-205
NC
miR-205
NC
miR-205
NC
E-cadherin
GAPDH

Figure 7

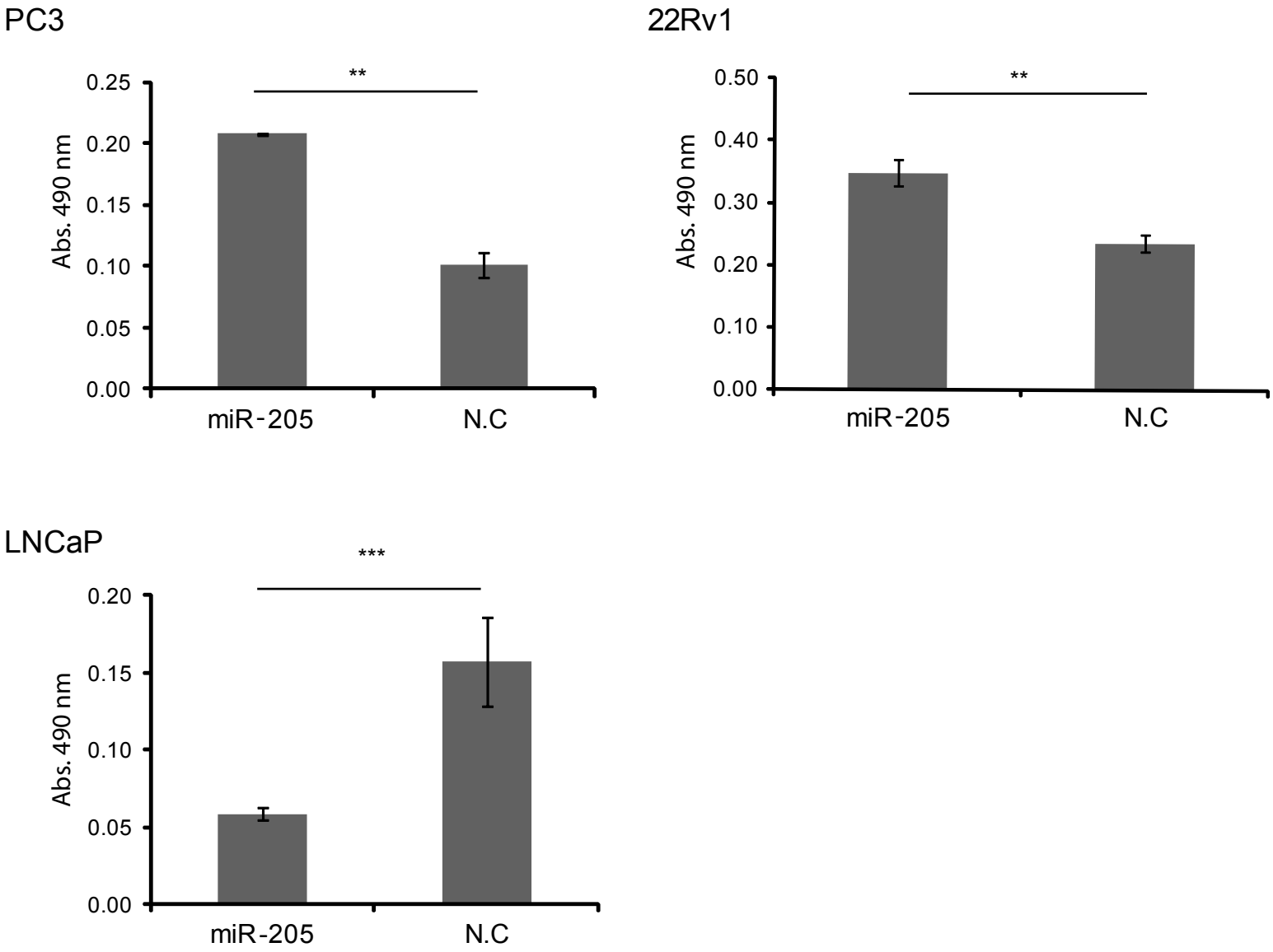
PC3
**
0.25
0.20
0.15
0.10
0.05
0.00
Abs. 490 nm
miR-205
N.C
22Rv1
**
0.50
0.40
0.30
0.20
0.10
0.00
Abs. 490 nm
miR-205
N.C
LNCaP
***
0.20
0.15
0.10
0.05
0.00
Abs. 490 nm
miR-205
N.C

Table 1.

Molecules fold change up-regulated		
Gene symbol	**Gene description**	**Fold change**
NR4A2	nuclear receptor subfamily 4, group A, member 2	5.6
EGR1	early growth response 1	5.1
NR4A1	nuclear receptor subfamily 4, group A, member 1	5.1
EPCAM	epithelial cell adhesion molecule	4.9
CCL20	chemokine (C-C motif) ligand 20	4.5
C1orf116	chromosome 1 open reading frame 116 , SARG	3.9
FGFBP1	fibroblast growth factor binding protein 1	3.9
CDH1	cadherin 1, type 1, E-cadherin (epithelial)	3.7
IL8	interleukin 8	3.7
EDN1	Endothelin-1	3.5
FOSB	FBJ murine osteosarcoma viral oncogene homolog B	2.9
JUNB	jun B proto-oncogene	2.3

Supplementary figure 1

miR-205

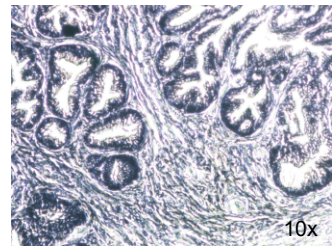

miR-205 + mimic

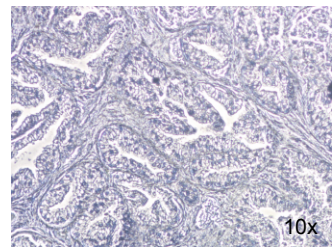

miR-205 + mimic
with 1 mutation

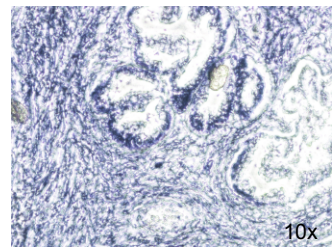

miR-205 + mimic
with 2 mutation

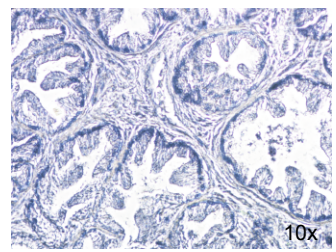

miR-205 + mimic
with 3 mutation

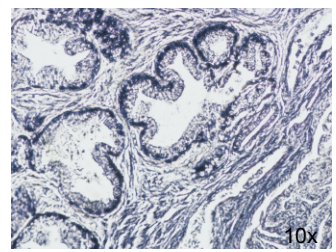

Supplementary figure 2

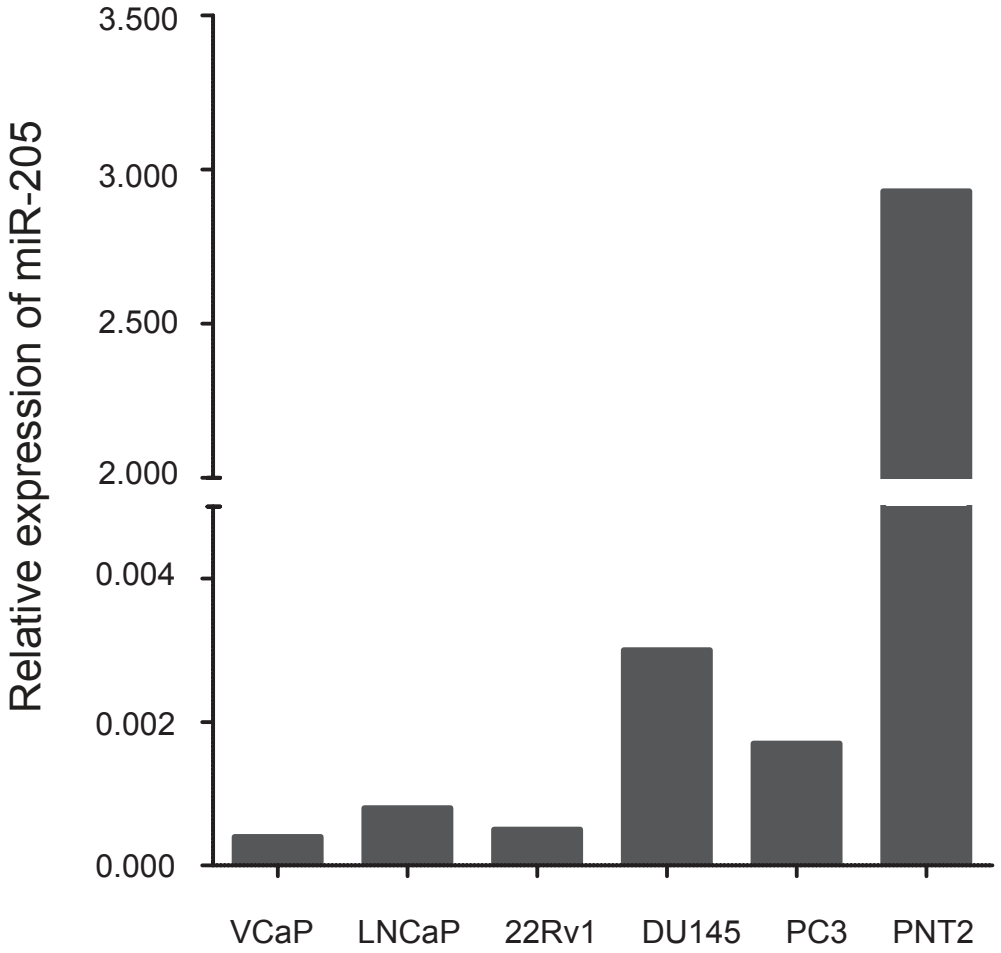

Supplementary figure 3

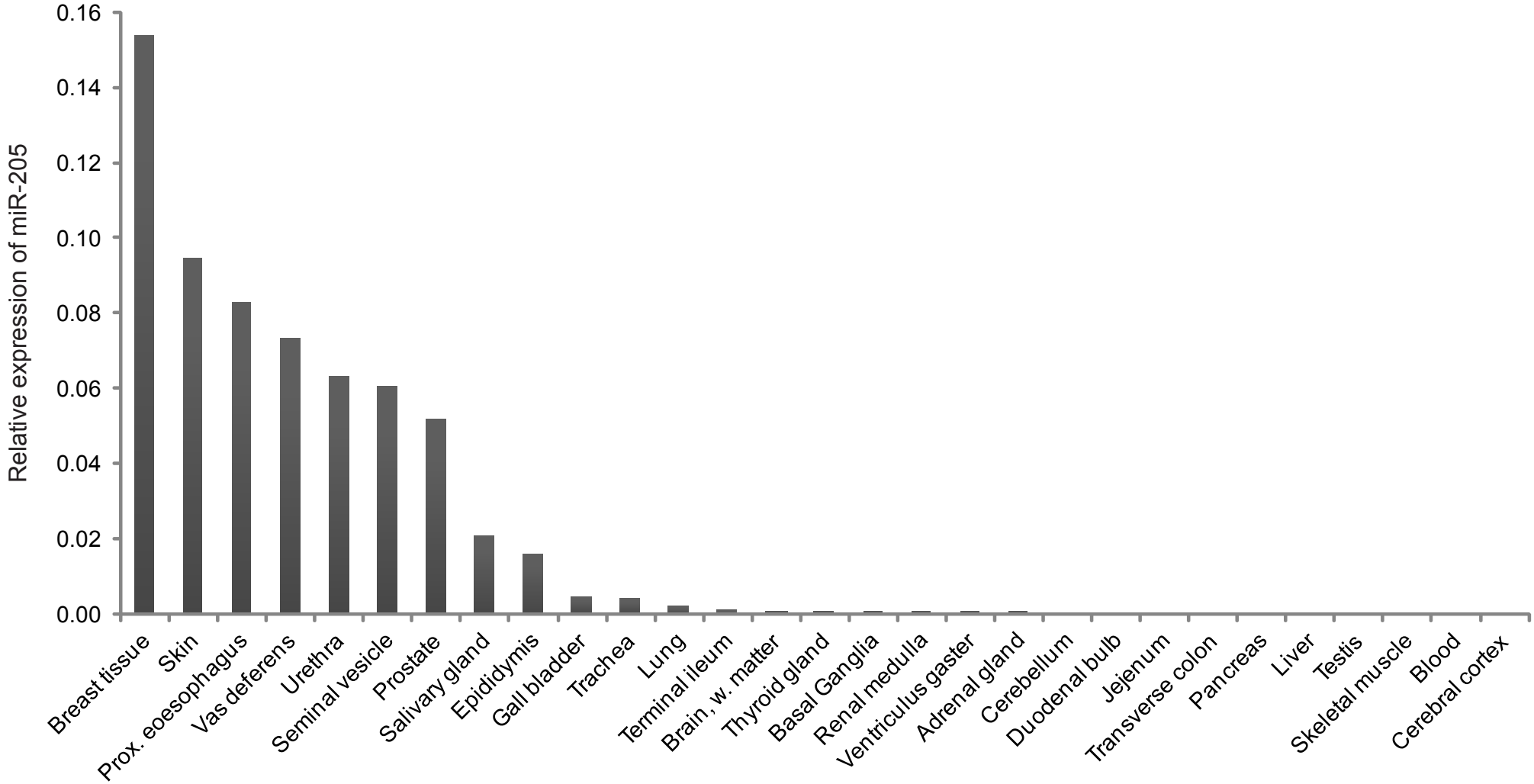

Tabel 1. Clinical characteristics of the study population.

	PCa (n = 49)
Age at TURP	
Mean (range)	76 (63 – 89)
WHO grade	
Grade I	5
Grade II	19
Grade III	25
PSA at diagnosis (n = 41)	
Median (range)	27 (0.2 – 428)
Occurance of metastasis* (n = 45)	
M0	17
M1	18
Mx	10
Androgen ablation treatment (n = 42)	
No	22
Ongoing	6
Fail	14
Cancer in tissue (%)	
Mean (range)	42 (5 – 90)

* **M0** = no metastasis; **M1** = having metastasis; **Mx** = not investigated since no suspicion at the time